The Reflectance of Single Cones in the Living Human Eye

Aristofanis Pallikaris,[1] *David R. Williams,*[2] *and Heidi Hofer*[2]

Purpose. Individual cones were imaged in the living human eye with the Rochester adaptive optics ophthalmoscope. In all eyes, there were large differences in the reflectance of different cones, even when all the photopigment was bleached. To help understand what produces this spatial variation, the investigators explored whether it is a static or a dynamic property of the cone mosaic.

Methods. Fully bleached cone images were acquired in three eyes with an adaptive optics system. Images were collected over a 10-minute period approximately every hour for 24 hours. The temporal variation in cone directionality was measured in one eye. Finally, the experimental data on the temporal variation of absorption were compared with findings in various models of reflectance.

Results. Cone reflectance changes over time appear to be independent from cone to cone. These temporal changes are present in all three cone classes. The spatiotemporal variation in cone reflectance is not caused by the spatiotemporal variation in the optical axes of cones. This, along with the modeling results, suggest that changes in the reflectance affect the light that passes through photopigment in the receptors rather than the stray light, and that the changes are related to the outer segment–retinal pigment epithelium (RPE) interface.

Conclusions. The reflectance of individual cones is a dynamic property of the mosaic. Changes can be observed over periods of minutes as well as many hours. The cause of the variation is not known but may be related to the process of disc shedding in receptors. (*Invest Ophthalmol Vis Sci.* 2003;44:4580–4592) DOI:10.1167/iovs.03-0094

Various techniques have been developed to characterize microscopic structures in the living human eye. Williams[1,2] developed a subjective technique based on photoreceptor aliasing to estimate cone spacing. Yellott[3] has demonstrated that the power spectra of in vitro images of the cone mosaic contains a ring of increased power centered on the origin, the radius of which is inversely proportional to photoreceptor spacing. Artal and Navarro[4] proposed that the average power spectra of retinal images obtained in vivo can also reveal this ring, and their method was subsequently used by Miller et al.[5] and Marcos et al.[6] Miller et al.[5] constructed a high-magnification fundus camera, showing that it is also possible to observe single cone photoreceptors in single images of small patches of retina. The subsequent correction of the optical aberrations of the eye with adaptive optics has greatly improved the ability to image single cones in vivo.[7–9] This technology has revealed the topography of all three classes of cones[10,11] and the angular tuning of individual cones in the living human eye.[9]

All studies of the cone mosaic in vivo show that the reflectance varies from cone to cone. Roorda (personal communication, September 2001), using the Rochester adaptive optics ophthalmoscope, observed that this spatial variation in reflectance changes from one day to the next. Wade and Fitzke,[12] observing single cones with a scanning laser ophthalmoscope, showed that the reflectance of cones can change even within a few seconds. The cause of this spatiotemporal variation has not been determined. In this study, we explored whether it is caused by differences in photopigment density or angular tuning and whether the site of the variation lies in front of or behind the cone outer segment.

Methods

Aberration Compensation

We obtained images of the cone mosaic in vivo with the second-generation Rochester adaptive optics ophthalmoscope. This instrument has been described elsewhere.[8] For the experiments described herein, it was improved by replacing the 37-actuator deformable mirror with a 97-actuator mirror. The subject's head was stabilized with a bite bar, and his or her pupil was dilated with tropicamide (2%). A Shack-Hartmann wavefront sensor measured the monochromatic wave aberration of the eye at 15 Hz. The wavefront sensor beacon was an 825-nm superluminescent diode with an irradiance of approximately 5 μW at the cornea. The distorted wavefront exiting the pupil was imaged on a square lenslet array with a focal length of 24- and 0.4-mm lenslet spacing. We used the direct slope control method[13] to transform wavefront sensor data into the appropriate commands to control the 97 actuators of the deformable mirror, which corrected the eye's monochromatic aberrations. Aberrations were corrected over a 6.8-mm pupil. Closed-loop correction continued until the root mean square (RMS) wavefront error fell below 0.1 μm or 12 loops had elapsed (800 ms), whichever occurred first.

Imaging

Immediately after correction was achieved, a retinal image was acquired by illuminating the retina with a 4-ms flash from a krypton arc flashlamp. The diameter of the flash was 1° at the retina. We controlled the spectral properties of the retinal imaging flash with interference filters of 550 or 670 nm (bandwidths, 10 and 40 nm full width at half maximum [FWHM], respectively). Except where otherwise specified, the flash irradiance at the retina was approximately 2.0 mW/mm^2 for 550 nm and approximately 0.11 mW/mm^2 for 670 nm. Although a 6.8-mm pupil was used for wavefront sensing and correction, a 6-mm pupil was used for retinal imaging to avoid correction errors at the edge of the deformable mirror. The light returning from the retina reflected off the deformable mirror and onto a charge-coupled device (CCD) camera that was conjugate with the retina. The CCD camera acquired retinal images with 512 × 512 pixels. The angle, subtended by a single CCD pixel at the retina, ranged from 6.62 to 7.34 sec of arc.

From the [1]Department of Biomedical Engineering and the [2]Center for Visual Science, University of Rochester, Rochester, New York.

Supported in part by the National Science Foundation Science and Technology Center for Adaptive Optics, managed by the University of California at Santa Cruz under cooperative agreement AST 9876783 and National Eye Institute Grants R01EY04367 and P30EY01319.

Submitted for publication January 29, 2003; revised May 28, 2003; accepted June 30, 2003.

Disclosure: **A. Pallikaris**, None; **D.R. Williams**, None; **H. Hofer**, None

The publication costs of this article were defrayed in part by page charge payment. This article must therefore be marked "*advertisement*" in accordance with 18 U.S.C. §1734 solely to indicate this fact.

Corresponding author: Aristofanis Pallikaris, Biomedical Engineering Department, University of Rochester, Rochester, NY 14672; apallik@med.uoc.gr.

It varied somewhat from subject to subject because the retinal image magnification changed somewhat with focus. We corrected our data for this difference in focus from subject to subject. Five subjects were used who were selected because of the clarity of their images of the cone mosaic. The research adhered to the tenets of the Declaration of Helsinki, and informed consent was obtained after the nature and possible consequences of the study were explained. Subjects' ages ranged from 20 to 26 years. We always imaged cones in the temporal retina of the right eye, 1° from the center of the fovea. At this eccentricity, the spacing between cones was 0.72, 0.83, 0.93, 0.91, and 0.88 (subjects AP, JG, TP, AL, and LD, respectively) minutes of arc, corresponding to approximately 6.52, 8.24, 7.60, 7.76, and 8.10 pixels, respectively, on the CCD.

To improve the image signal-to-noise ratio, we collected several images for each experiment, dark subtracted with an average of 20 dark images, registered with subpixel accuracy, and added together. In several experiments, we estimated the light reflecting from a single cone by averaging the reflectance across the 3 × 3-pixel region closest to the center of each cone.

Definition of Reflectance

We use the term "reflectance" throughout the article to refer to the fraction of light reflected from particular cones. Reflectance is defined as the ratio of the irradiance at the CCD camera when a subject's retina is in the optical system to the irradiance at the CCD camera when the eye is replaced with a 100% reflective mirror located in the pupil plane. This mirror directs all the light that would otherwise have entered the eye back onto the CCD camera. Therefore, the factors that reduce the reflectance from unity are only those associated with the eye. These include the double-pass light losses through the optic media, the low inherent reflectivity of the fundus, and the light lost due to retinal backscatter at a solid angle larger than that subtended by the eye's pupil. In both imaging situations, the entrance pupil of the krypton flash lamp was 4 mm, to ensure the same flashlamp irradiance, and the limiting aperture of the system was a 6-mm artificial pupil that was placed in the imaging path of the adaptive optics ophthalmoscope. We used neutral-density filters when the mirror was located in the pupil plane, to ensure that there was no saturation in the imaging camera. The mirror images were also dark subtracted by an average of 20 dark images, and an average of 3 × 3 pixels regions were used to measure the average irradiance of the mirror onto the CCD camera. Thus, the term "reflectance" was defined as the ratio of the irradiance onto the CCD camera of the cones to the average irradiance of the mirror.

Photopigment Bleaching

Some experiments required imaging the cone mosaic after bleaching of cone photopigment. Subjects viewed a diffuser back-illuminated by a tungsten-halogen lamp for 30 seconds. The light was filtered by a 550-nm interference filter (bandwidth, 75 nm FWHM) as well as a UV blocking filter. The bleaching light subtended 1.25° at the retina and had a retinal irradiance of 3×10^6 trolands. Based on the bleaching equation of Alpern et al.,[14] we expected this light to bleach 97% of the medium (M) and long (L) wavelength-sensitive cone photopigment. Images were collected within 3 seconds of the bleaching exposure. Images acquired with the eye fully dark adapted were preceded by 5 minutes in darkness.

Results

Temporal Variation of Reflectance of Cone Photoreceptors

We conducted several experiments to determine whether the temporal variation in cone reflectance follows a systematic pattern. We collected fully bleached retinal images over a 10-minute period approximately every hour for approximately 24 hours in three different subjects. We used fully bleached images to ensure that variations in pigment absorptance in space or time did not influence measurements of cone reflectance. Images were acquired on two different days in one of the subjects. The subjects followed their normal schedules during the day, though sleep was disrupted at night. A minimum of three fully bleached images were registered and summed for each hourly sample. Because we were interested in the changes in reflectance over time and not the average reflectance, we subtracted the reflectance of each cone by its time-averaged reflectance. We computed the autocorrelation of each cone signal by computing the sum of the cross products of the zero-centered cone reflectance with time and its time-shifted version. We then averaged the autocorrelation functions of all the cones to estimate how rapidly cone reflectance changes over time and whether there is any fundamental periodicity to these changes. An advantage of averaging autocorrelation functions of individual cones is that it reveals a periodicity in cone reflectance even if the phase of this periodicity is not systematic across cones. Finally, to assess the effect of variations in imaging focus on the autocorrelation functions, we calculated the RMS contrast of the images over the 24-hour period.

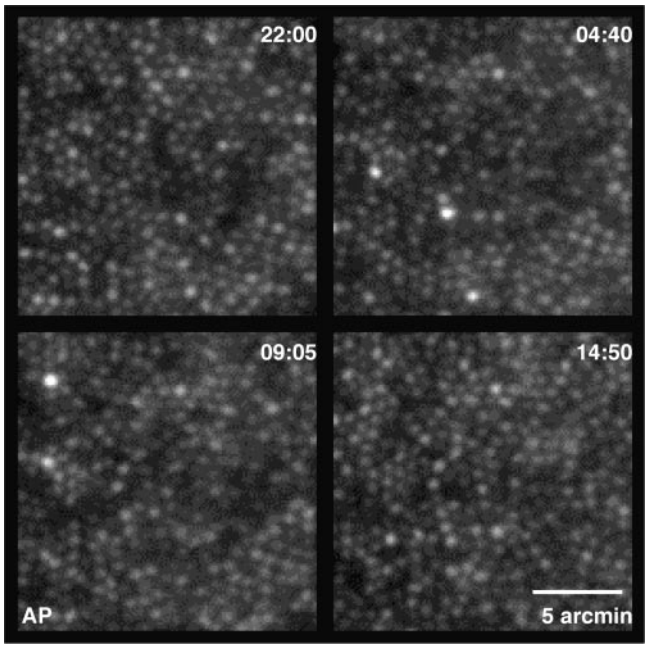

Figure 1. Twenty-four-hour imaging experiment. A composite set of four images taken during a 24-hour period. Each image represents the registered sum of at least three fully bleached images taken approximately every hour within a 10-minute interval (the time is indicated on the *upper right corner*). All images were taken at the same location of 1° eccentricity from the center of the fovea. The spatial variation is unsystematic, yet cones change their reflectance from image to image.

Figure 1 shows a composite of images taken at various times over the 24-hour period in one of the subjects. Some cones increased their reflectance and others decreased their reflectance in a haphazard pattern. Figure 2 shows the reflectance of four cones divided by the images' mean reflectance, which spans the range of behavior in the population of 948 cones we studied. For display purposes, the reflectance of cones in Figure 2 was normalized by the corresponding average reflectance of each sampled image. Cones 1 and 2 showed the largest changes in reflectance, with cone 1 changing by a factor of 3.5 over the 24-hour period, whereas cones 3 and 4 changed the least. Cones may change their reflectance gradually with time (cone 1) or change abruptly (cone 2). Figure 3 shows the autocorrelation plots for two of the three subjects. The results for the third subject were similar. These plots show a high

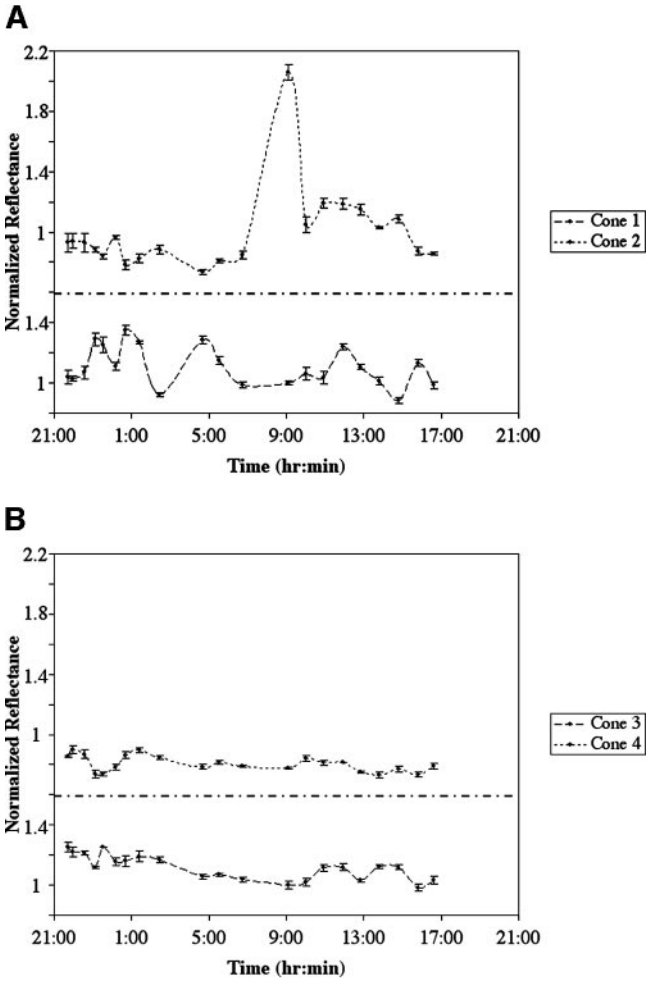

FIGURE 2. Representative reflectance of cones. The reflectance of four cones as observed over a 24-hour period. Cones have been displaced by 1 unit with respect to the first cone of each graph for clarity. The reflectance of cones may change gradually or abruptly by as much as a factor of 3.5 (**A**) or may stay constant throughout the experimental period (**B**).

correlation for times of an hour or more, declining to zero after approximately 6 hours (373 ± 6 minutes). All three subjects showed a negative correlation after approximately 6 hours that reached a minimum at 12 hours and then returned toward zero. This negative lobe indicates that if a cone is bright (or dark) at any particular time, there is a slight tendency for it to be dark (or bright) approximately half a day later. Unfortunately, for the benefit of our subjects, we chose not to continue the experiment beyond 24 hours, and so we do not know how the function would behave beyond that time. However, the autocorrelation coefficients do not show a strong tendency to rise above zero at 24 hours, as one would expect if the reflectance changes had been governed by a circadian process. We examined the mean reflectance of all the cones as well as the variance of the reflectance as a function of time. Neither of these showed any indication of circadian periodicity of reflectance. Taken together, these findings suggest that the cones brighten and darken largely independent of each other. Moreover, the RMS contrast of the images showed only a small variation over time. The SD of the RMS contrast divided by its mean is 0.06, on average, for all subjects, indicating a small effect on the autocorrelation function. Although a change in focus of the images would drive the cone reflectances toward the mean reflectance, these changes are not large enough to explain the relative changes in reflectance that we observed among the cones.

We cannot rule out the possibility that a circadian rhythm exists but that it was perturbed in our experiments by the procedure itself, such as the frequent exposure to bleaching lights throughout the experiment. We conducted one experiment that showed that bleaching per se does not influence cone reflectance immediately after bleaching. We examined the spatial variation in cone reflectance at 670 nm, where none of the cone photopigments have appreciable absorptance. Even the L pigment would be expected to modify the reflectance of a cone by only 0.002 at this wavelength. We alternated the collection of 10 fully bleached images and 10 dark-adapted images from the same location within a 2-hour period and examined the reflectance variation of cones. The average reflectance was not subtracted in this case.

Figure 4 shows the registered sum of the fully bleached and dark-adapted images, and Figure 5 plots the histograms of the intensities of the cones. The mean ± SD of the reflectances of the cones was $5.23 \pm 0.56 \times 10^{-3}$ for the fully bleached image and $5.23 \pm 0.57 \times 10^{-3}$ for the dark-adapted image. The two distributions are not statistically different according to the standardized student's *t*-test ($P > 0.05$). Moreover, the correlation coefficient between the two images is 0.85. This suggests that bleaching photopigment does not by itself introduce

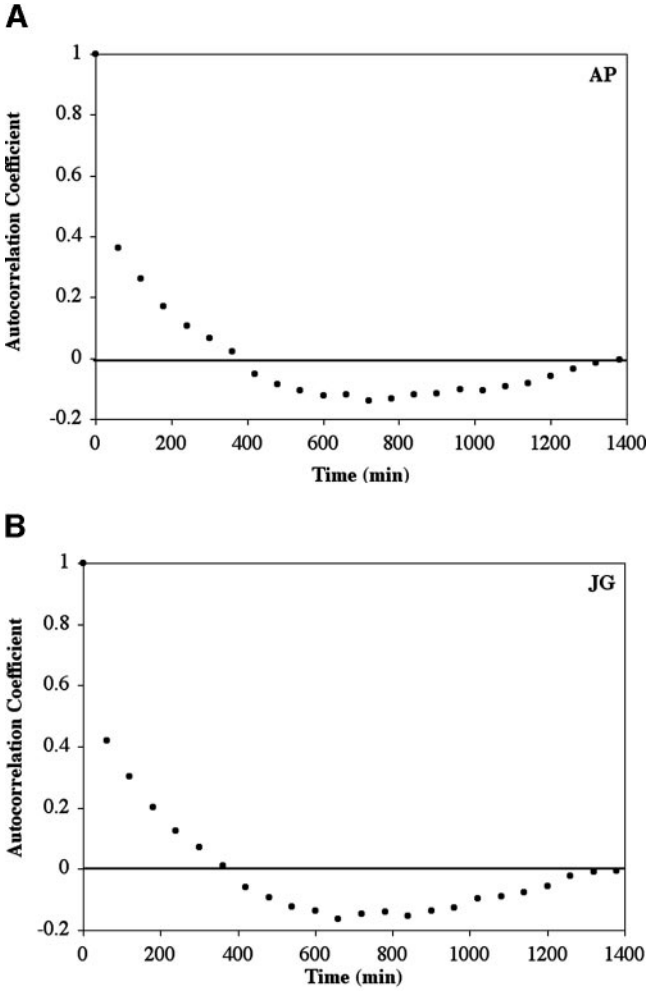

FIGURE 3. Average autocorrelation of reflectance of cones with time in subjects AP (**A**) and JG (**B**). *Circles* represent the autocorrelation coefficients of the zero-centered reflectance signals as a function of time averaged over all cones. The mean reflectance over time of each cone was subtracted.

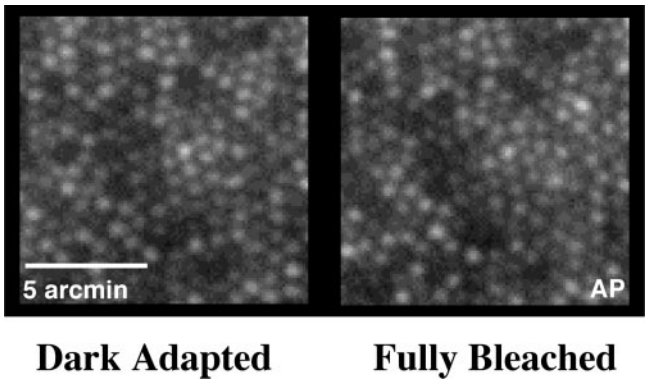

FIGURE 4. Fully bleached and dark-adapted images. Each image is the registered sum of 10 retinal images taken from the same subject (AP) and at the same retinal location (1° eccentricity from the center of the fovea) within a 2-hour interval using a 670-nm interference filter. The contrast of each image has been maximized for display purposes.

changes in the intrinsic reflectance of cones, at least immediately after bleaching. We have not explored whether bleaching has any longer term impact on cone reflectance.

We supplemented experiments in which images were taken every hour with experiments in which images were acquired as rapidly as once every 30 seconds over periods of up to 3 hours to see whether rapid changes also occur as had been reported by Wade and Fitzke.[12] We examined the absolute reflectance of single cones and in agreement with their observations, we also sometimes saw abrupt changes. As indicated in Figure 6, cones can sometimes change reflectance by a factor of 2.4 in 13 minutes. These rapid changes occur infrequently.

Spatial Extent of the Temporal Variations of Cone Reflectance

The spatial extent over which the temporal variations in cone reflectance are correlated indicates the spatial dimensions of the process that is responsible for them. For example, if neighboring cones exhibited a similar temporal pattern of reflectance, it would suggest that the cause of the phenomena is not localized within a single cone. Casual inspections of time-lapse movies (see http://www.iovs.org/cgi/content/full/44/10/4580/DC1) we have made of changes in cone reflectance over 24-hour periods suggest that the changes are largely confined to single cones and are not obviously correlated among nearby

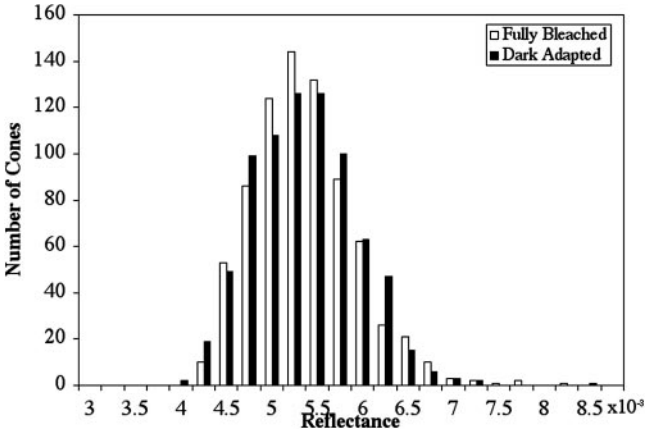

FIGURE 5. Histograms of the reflectances of the dark-adapted and fully bleached images. The histograms plot the reflectances of 766 cones. A 670-nm interference filter was used for image acquisition.

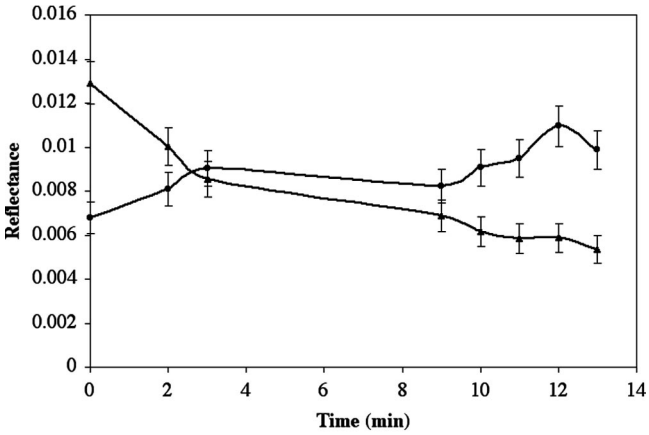

FIGURE 6. Rapid changes in reflectance. The graph shows two cones changing their reflectance within a 13-minute period. One cone exhibited an increase in reflectance by a factor of 2.4, whereas the other exhibited a decrease in reflectance by a factor of 1.6. Rapid changes in reflectance may occur but are infrequent.

cones. We quantified this by calculating the correlation of reflectance over a 24-hour period between pairs of pixels and plotting the correlation coefficient as a function of angular separation between pixels, as shown in Figure 7. For this calculation we did not perform any subtraction or division on the cone reflectances. We then compared this function with the spacing between cones as well as the radial average point-spread function (PSF) after adaptive optics correction for each subject.

The correlation coefficient decreases as a function of angle to zero at a rate that is slower than the decline in the intensity of the eye's PSF. Nonetheless, most of the decrease occurred in less distance than that to the nearest neighboring cones. In all three subjects, the correlation coefficient decreased to 0.16 ± 0.05 at a distance equal to the cone distance. Cone distance was defined as the reciprocal of the modal spatial frequency in the power spectrum of the cone mosaic, which corresponds to the distance between rows of cones (and not center-to-center spacing) in a triangularly packed mosaic,[15] times the square root of two. The correlation did not decrease entirely to zero, even at larger distances, providing some support for the notion of a cause for the cone reflectance variations at a larger spatial scale than a single cone. This may be partly due to light scatter in the eye that is not captured by the wavefront sensor from which the PSF was estimated. We cannot exclude a weak large-scale retinal component as well. Nonetheless, the rapid initial decline implies that the main cause of the reflectance change is localized in single cones.

Temporal Variation in Each of the Three Cone Classes

We performed an experiment to determine whether the temporal variation in cone reflectance is specific to a subset of the three classes of cone, or whether it is a general property of all cones, regardless of the pigment they contain. We examined this question in a single subject in whom we had previously classified each cone in a patch with the method described by Roorda and Williams[10] and Roorda et al.[11] In short, retinal densitometry was combined with high-resolution retinal imaging, and individual cones are classified by comparing fully bleached images with either dark-adapted images or images in which the cones have been selectively bleached with monochromatic light. Short-wavelength–sensitive (S) cones were distinguished by comparing fully bleached and dark-adapted images, whereas L and M cones were identified by comparing

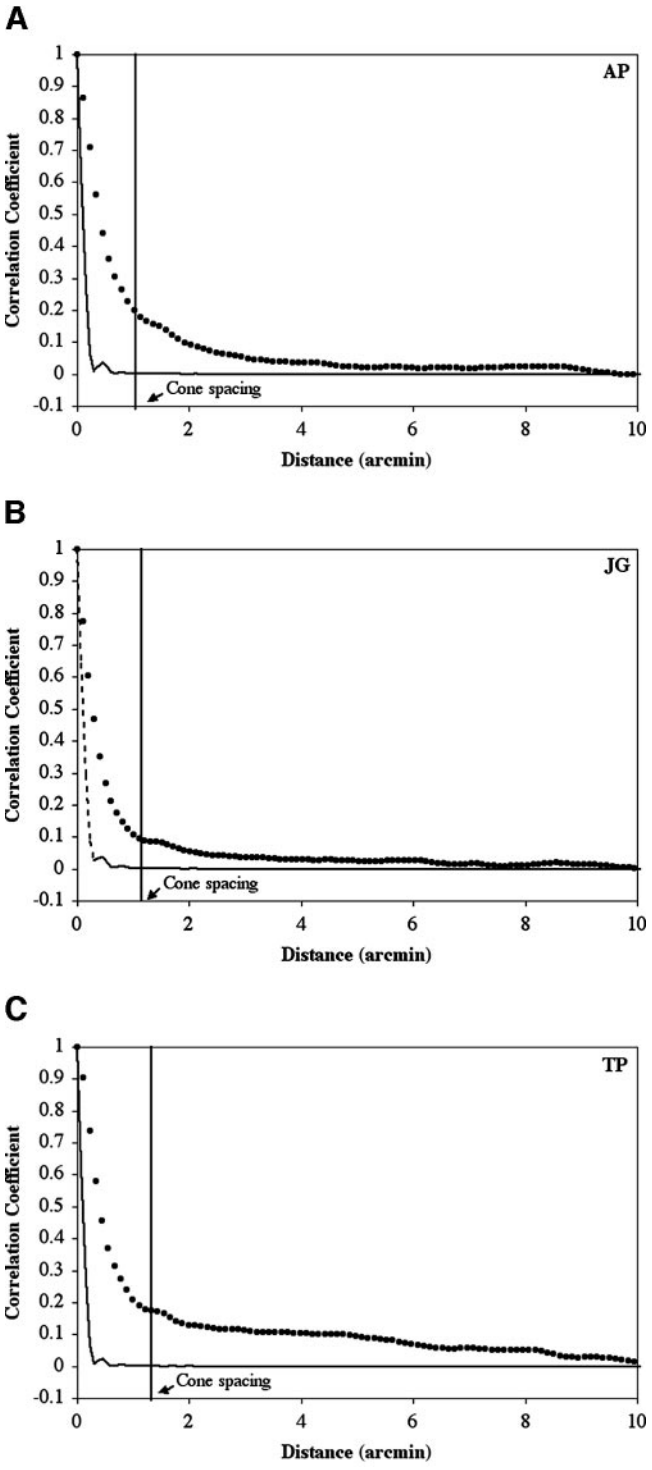

FIGURE 7. Spatial correlation over the 24-hour period. *Circles*: correlation coefficient between pairs of pixels as a function of distance between them; *dashed curve*: PSF after adaptive optics compensation. The cone sizes of (**A**) AP, (**B**) JG, and (**C**) TP are indicated on the graphs (*arrows*). The correlation coefficients decreased as the distance between pixels increased.

dark-adapted images with 650- or 470-nm bleached images, respectively. The S cones were identified because they absorb negligible light at 550 nm and therefore exhibit the same reflectance in both the dark-adapted and fully bleached images. Once the cones were classified, the data for the 24-hour experiment were used to compute the temporal variance of each cone. Figure 8 shows the retinal mosaic and the histograms of the temporal variance in reflectance over the 24-hour period for each of the three cone classes. Again, we did not perform any subtraction or division on the cone reflectances. The log-normal fits are the same shape, suggesting that the temporal variation is not specific to a particular cone class and that all three cone classes have the same amount of temporal variation.

A Role for Angular Tuning in Cone Reflectance Changes?

It has been known for some time that cone photoreceptors have relatively narrow angular reflectance functions, returning much more of the incident light toward a point near the center of the pupil than toward the pupil margin.[16–21] This phenomenon is closely related to the Stiles-Crawford effect (SCE), which describes the variation in the visual effectiveness of light entering through different locations in the pupil.[22,23] In fact, both the angular reflectance function (cone directionality) and the relative luminous efficiency as a function of entrance pupil position (SCE) exhibit the same peak location.[24] It has long been suspected, and recent evidence has nicely confirmed, that cone directionality is plastic, so that the cones can orient themselves toward the functional pupil center.[25,26] Changes in cone orientation could be responsible for the changes in single cone reflectance we observed. Alternatively, the directionality of the cone could remain the same and the cone's reflectance change could be caused by intrinsic changes within the cone or its immediate surroundings.

To distinguish between these two hypotheses, we measured the directional sensitivity of individual cones with the method introduced by Roorda and Williams.[9] We translated an artificial 1.5-mm entrance pupil in random sequence over five positions along the horizontal and vertical meridian in the pupil. For each illumination position in the pupil, we kept the exit pupil fixed and centered on the peak reflectance. The exit pupil used for imaging the retina was always 6 mm in diameter. Changing the illumination angle on the retina also produced small changes in the irradiance due to nonuniformities in the source, which were removed by normalizing the reflectance by the measured irradiance of the krypton flash lamp for each position. The flash irradiance at the central position of the entrance pupil was approximately 0.1 mW/mm^2. We registered and summed eight fully bleached images for each pupil entry location. Furthermore, we measured the reflectance (with the mean reflectance of the image not subtracted) of a series of cones at 1° eccentricity for each entrance pupil

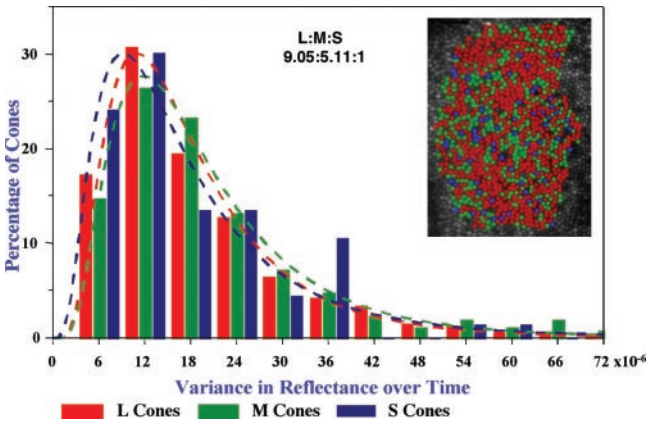

FIGURE 8. Histogram of variance in reflectance over time for the three cone classes. The histograms of the three cone classes are shown for one of the subjects as well as the best log-normal fits (*dashed lines*). The three log-normal fits exhibit similar trends. The L to M to S wavelength cone ratio is also indicated.

position and fitted them by using a least-squares procedure with the Gaussian angular tuning function

$$I = c + Ae^{-(\vec{s}-\vec{s}_{peak})^2/2\sigma^2} \quad (1)$$

where c is the diffused component of the reflectance of the cone, A represents the directional peak reflectance of the cone, s_{peak} is the peak position of the reflectance at the pupil position, and σ is the spread of the Gaussian intensity profile. We repeated the experiment twice on the same eye on two different days, to examine any cone directionality changes over time that could account for the changes in cone reflectance.

Figure 9 shows a composite of images taken at five different entrance beam locations in the vertical and horizontal directions. These images reveal the directional sensitivity of cone reflectance through the decrease of the intensity of the images with increasing eccentricity of the illumination beam in the pupil. Note that the pattern of spatial variation of intensity is preserved, suggesting that there is small disarray in the optical axes of the cones within each day. Furthermore, Figure 10 shows the central images acquired at the same location and in the same eye on the 2 days, as well as the Gaussian tuning function of a brightening and a darkening cone. This example shows a negligible change in the cone's pointing direction (and the breadth of tuning as well) across the 2 days, but a large change in the intrinsic reflectance, indicated by the change in height of the tuning curve. Similar results were found in all 658 cones examined. The SD of the difference in the cone-pointing position in the pupil was only 0.12 mm—very small compared with the 6-mm pupil over which images were acquired. Indeed, it is only 1.3 times larger than the SE of estimating the peak. Therefore, most of this variation is probably measurement error and not real shifts in cone position.

We compared the effect of shifts in directional sensitivity and intrinsic changes in this cone population as follows. To estimate the effect of directional sensitivity by itself, we nor-

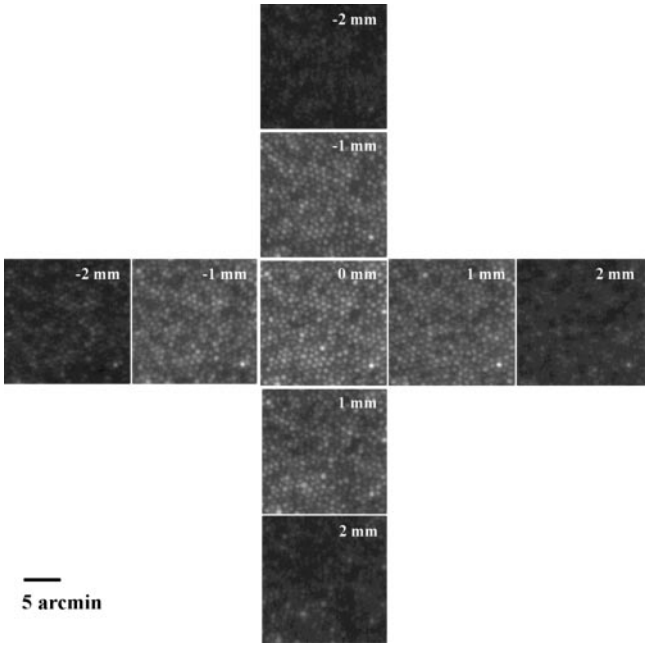

FIGURE 9. Cone directionality. The images represent the registered sum of the fully bleached images for each of the nine entrance pupil illumination positions. Each image is of the same patch of retina. The number in the *top right* of each image represents the artificial pupil position in relation to the center of the illumination beam. The intensity of the images decreases with distance away from the central image, yet the spatial variation remains the same.

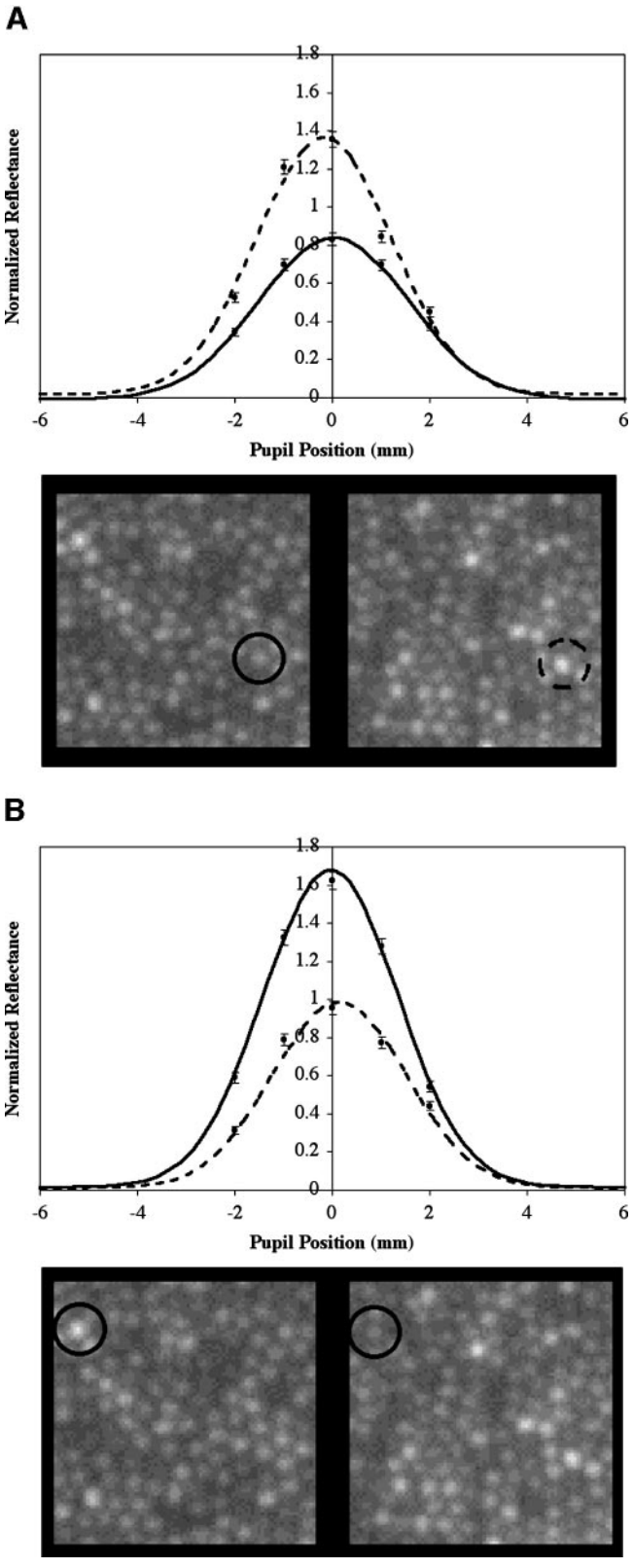

FIGURE 10. Temporal variation in the directionality of a brightening cone and a darkening cone. The images shown represent the central images of the optical Stiles–Crawford experiment for the two different days. Each image is the registered summed of five fully bleached images taken of the same retinal patch. *Circles*: the same brightening (darkening) cone, and the graphs illustrate the Gaussian profile of the cones for the 2 days. The zero position corresponds to the SC peak of day 1 (**A**) and day 2 (**B**). The graphs illustrate that cone directionality remained essentially constant over time.

malized to unity the peak of the Gaussians that were fit to each cone on days 1 and 2. This removed any intrinsic reflectance changes across the 2 days. Next we computed the difference in reflectance that would have been observed through the 6-mm imaging pupil, given the changes in that cone's directionality. We then formed a distribution of these difference data across all cones. This distribution had a mean very close to zero. The SD of this distribution is a measure of how much shifts in pointing direction changed the apparent receptor reflectance. This SD was 0.02, which is very close to zero, indicating a small change in reflectance due to directionality.

To estimate the impact of intrinsic changes in cones, we took the difference in the peaks of the Gaussians fit on days 1 and 2. By choosing the peaks, we deliberately ignored the effects of changes in pointing direction, focusing instead on intrinsic changes. The SD of the distribution of peak differences was 0.2, which is 10 times greater than that associated with pointing-direction effects. In other words, changes in pointing direction over time were very small, were probably within the noise of our measurements, and had negligible impact on the changes in cone reflectance that we observed.

These changes must be a consequence of intrinsic changes either within cones or in the milieu immediately proximal to single cones. Figure 11 shows the relationship between the changes in reflectance and the changes in the directional component and the diffuse component of the reflected light, both within a day and across days. It is clear from Figure 11 that whatever the physical cause of the change in cone reflectance, it affects the directional component of the reflected light and has little or no effect on the nondirectional background light reflected from the retina, which seemed to be rather small to begin with. This implies that the cause of the temporal variation in reflectance is located at a site within or very close to the receptor itself, so that it can influence only the intensity of the light guided by the receptor and not the background light.

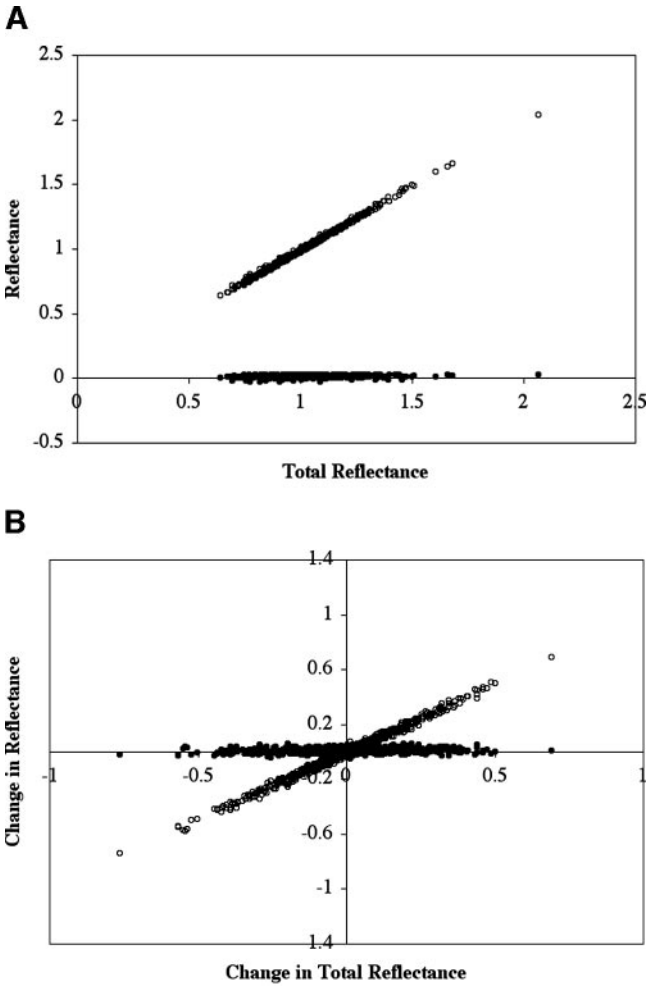

FIGURE 11. Changes in reflectance were related to the directional component of light. (**A**) The directional (○) and diffused (●) reflectances with respect to the total reflectance; (**B**) changes in the directional (○) and the diffused (●) reflectances with respect to the changes in the total reflectances The changes in reflectance are related to the changes of the directional component of light and not the changes of the diffused component.

Relationship between Cone Absorptance and Reflectance

In the dark-adapted retina, a possible contributor to the spatial variation in cone reflectance could be differences from cone to cone in the absorptance of the photopigment. Although cone outer segments at any eccentricity have roughly similar lengths at a fixed eccentricity, they could differ in the density of pigment within them. If this were true, then one would expect the spatial variation to increase when the photopigment is regenerated. We imaged one subject's eye on two different days, acquiring 20 dark-adapted images and 20 fully bleached images within a 2-hour interval. Throughout this interval, image acquisition alternated between dark-adapted images and fully bleached images. Again, the S cones were identified because they absorb negligible light at 550 nm and therefore exhibit the same reflectance in both the dark-adapted and fully bleached images. We removed them from our data analysis.

Figure 12A shows histograms of the reflectances (with the mean reflectance of the image not subtracted) of the remaining dark-adapted and fully bleached M and L cones. On each of the 2 days, the mean reflectance of cones of the fully bleached image was 1.9 times greater than that of the dark-adapted image, because of the absorptance of photopigment. However, dark adaptation did not increase the spatial variation in cone reflectance when this variation is expressed as a fraction of the mean reflectance. Specifically, the SD divided by the mean for the dark-adapted images averaged over the 2 days was 0.18 and that of the fully bleached images was 0.17. This is illustrated in Figure 12B, in which both distributions have been normalized to the same mean. These were not significantly different, suggesting that spatial variations in cone pigment absorptance do not greatly increase the overall spatial variation in cone reflectance. This is not to say that nearby cones do not differ in the density of the photopigment they contain, but that these variations are small compared with variations in the cone reflectance.

The direct assessment of the amount of the visual pigment in vivo is based on the comparison between the reflectance of the fully bleached image and the dark-adapted image, and is calculated as

$$A = 1 - \frac{R_d}{R_b} \qquad (2)$$

where A is the absorption of light by the visual pigment, R_d is the reflectance of the dark-adapted image, and R_b is the reflectance of the fully bleached image. This calculation yields the apparent absorptance in each cone. The true cone absorptance is higher than the measured variation, because only a fraction of the light that arrived at our CCD from the location of a cone actually passed through the photopigment. The remaining fraction is stray light that could arise from the cornea and lens, the retina lying in front of the photopigment, or light that travels in the receptor interspaces without passing through photopigment on either the first or second pass. This is a familiar

problem in retinal densitometry[27–29] that influences cone-resolved retinal densitometry as well. The measurements in our study are similarly contaminated. For example, the apparent double-pass absorptance of cones in AP, TP, and LD is 0.46, 0.32, and 0.26, respectively. However, we expect to see a double-pass absorptance of 0.92 based on an outer segment length of 36 μm[30] and a specific optical density of 0.016 μm^{-1}.[31] However, the 4-ms krypton flash lamp exposure bleaches approximately 40% of the outer segment pigment of the cones in the dark-adapted images. This bleaching reduces the amount of the apparent double-pass absorptance expected to approximately 0.69. Nonetheless, on average, this value is still 2.1 times higher than the experimental double-pass absorptance of cones in the three subjects. In our particular imaging situation, the stray light from the cornea and lens was negligible because of the high retinal magnification we used. Moreover, our choice of imaging within the fovea reduced the amount of light returning from retinal layers in front of the photoreceptors. In addition, our use of a 550-nm interference filter maximized the fraction of light returning from photoreceptors.[32] The absence of a substantial uniform background in the angular tuning measurements for observer AP, presented earlier, show that in his eye, this stray light seemed to be directional, in a fashion similar to the light that passes through the receptors. However, we did not obtain estimates of the cone reflectance at eccentricities in the pupil larger than 2 mm, which made it difficult to assess the size of the diffuse component. If the reflectance functions were truly Gaussian functions of pupil position, then our fits suggest that there was almost no diffuse component. This conclusion conflicts with findings in previous studies,[18–21] and we therefore cannot reject the idea that there is in fact a somewhat larger diffuse component and that a Gaussian is not a good description of the data.

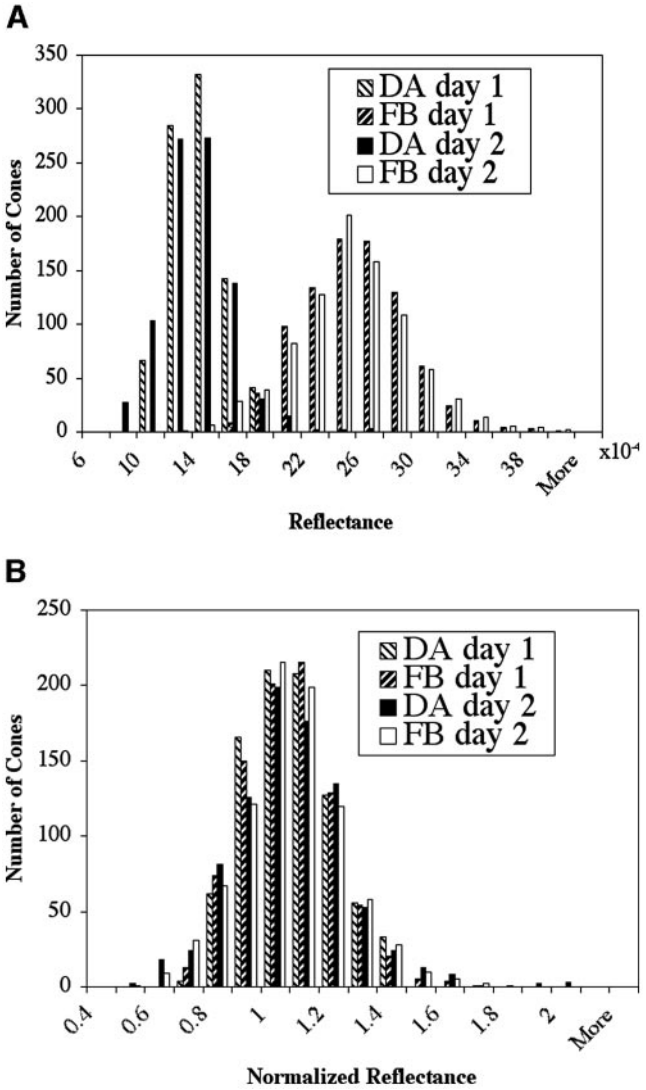

FIGURE 12. Histograms of the reflectances of the dark-adapted and fully bleached images. Both fully bleached and dark-adapted images were acquired on two different days in the same eye. (**A**) The histograms plot the reflectances of the 866 L and M cones. (**B**) The histograms plot the same distributions normalized by their mean intensity.

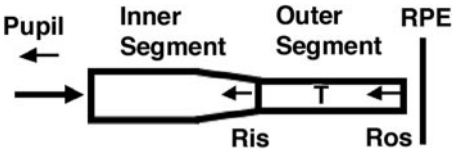

FIGURE 13. Simple reflectance model. Reflection can be attributed to the first surface of the outer segment or the outer segment–RPE interface. Changes in the intensity of the directional component of light may result from changes in the reflectance R_{is} or R_{os}.

We constructed models of retinal reflectance that use estimates of the apparent cone absorptance and how they depend on cone reflectance to clarify the site in the retina where the changes in cone reflectance occur. Light returning from the retina in our adaptive optics imaging system can arrive at our detector from several sources, any of which could be responsible for the fluctuations in cone reflectance we observed. The simplest reflectance model, proposed initially by Rushton[27] and Ripps and Weale,[33] assumes that light is reflected from a layer just behind the cone outer segments, such as the retinal pigment epithelium (RPE). This reflected light is coupled to the cone's outer segment to provide the directional component of the reflected light at the pupil. Figure 13 shows the simple model including the reflection of light from interface between the inner and outer segment (R_{is}) and the reflection from the interface between the outer segment and the RPE (R_{os}). In this model, we assume that the light corresponding to R_{is} or R_{os} is directionally guided back toward the pupil, as implied by the low apparent absorptance combined with the absence of a uniform background in subject AP's pupil. As discussed earlier, we do not know whether this conclusion is valid, and leave open the possibility that some of the stray light under these same experimental conditions is unguided. Whether the stray light is guided or unguided does not change the specific conclusions we will propose based on our model. Equations 3, 4 and 5 provide the basic mathematical relationships that describe optical absorption measurements as a function of the various reflectances of the model.

$$R_b = (R_{is} + (1 - R_{is})R_{os}) \quad (3)$$

$$R_d = (R_{is} + (1 - R_{is})R_{os}T) \quad (4)$$

$$A = \frac{(1 - T)(R_b - R_{is})}{R_b}. \quad (5)$$

R_{is} represents the reflectance of the inner segment–outer segment interface, R_{os} represents the reflectance of the outer segment–RPE interface, and T is the double pass transmittance of light that propagates twice within the outer segment.

In this model, either R_{os} or R_{is} could vary across different receptors or change in time within a single receptor. To decide which source of light actually varies in space and time, we

compared model predictions with experimental data on the relationship between apparent absorptance of a cone and its reflectance. Figures 14 and 15 show examples of the model predictions. The parameter for the different curves is the ratio of R_{os} to R_{is}. Figures 14A and 15A show how the absorptance of different cones should vary with reflectance at a single point in time. If R_{is} varies across the mosaic (Fig. 15A), then absorptance should be negatively correlated with reflectance, because the brighter the cone the larger the fraction of light that did not pass through pigment. However, if R_{os} varies across the mosaic (Fig. 14A), then absorptance should be positively correlated with reflectance, because the brighter the cone the larger the fraction of light passing through pigment. Figures 14B and 15B show the model predictions for a single cone, the reflectance of which changes over time. As in the case of spatial variation, the model predicts a negative correlation for variation in stray light within a cone (Fig. 15B), but a positive correlation if the site of variation is in a location that influences the amount of light passing through photopigment (Fig. 14B).

We tested these alternatives experimentally by acquiring both fully bleached and dark-adapted images in three eyes on two different days. The subjects dark adapted for 5 minutes before the acquisition of a dark-adapted image and bleached the retina for 30 seconds before the acquisition of a fully bleached image. Two fully bleached images were acquired immediately after the dark-adapted image, and a total of 20 sets were collected for each day. We registered and summed the dark-adapted images and the fully bleached images separately, and we measured the apparent absorptance by the pigment of the cones, using equation 2. We also measured the reflectance of the same cones for the two different days from the fully bleached images. Again, the mean reflectance of the image was not subtracted from the reflectance of the cones for this experiment. Figure 16A shows the measured absorption as a function of cone reflectance for each subject. Filled and unfilled symbols show the results for the first and second days, respectively. Figure 16B shows, for each cone in each subject, the change in absorptance as a function of the change in reflectance from the first to the second day. Note that all the six graphs (Figs 16A–F) show a positive correlation between absorptance and reflectance. This clearly rejects the possibility that differences in cone reflectance across space and time are caused predominantly by changes in the amount of stray light that does not pass through photopigment. The data favor the alternative that the variations in cone reflectance are caused by a factor that affects primarily the light that passes through the cone photopigment.

On the assumption that all the variation in cone reflectance is due to changes in R_{os}, we estimated the value of R_{is} that

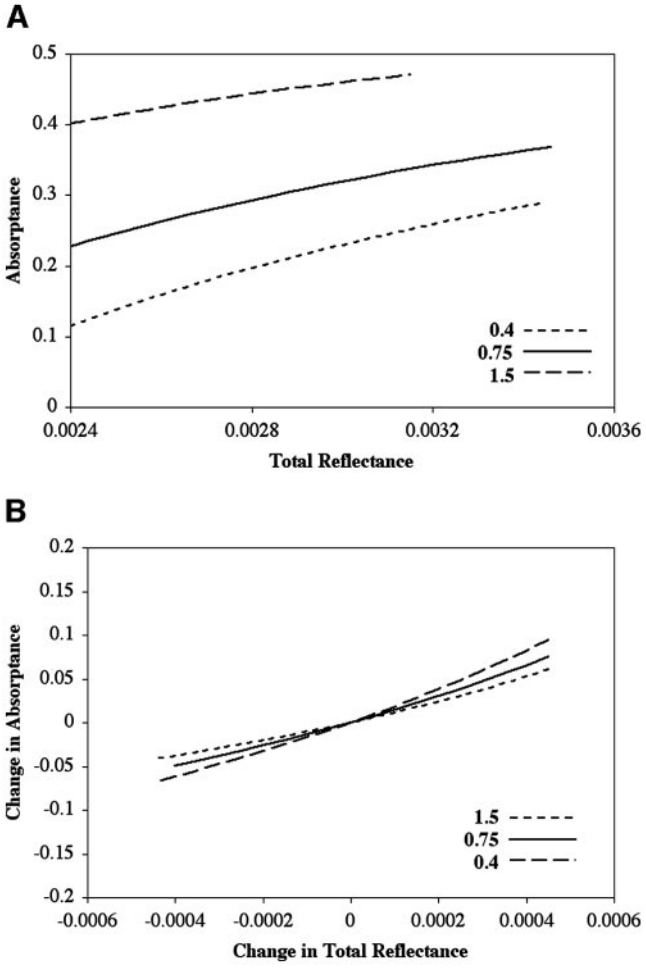

FIGURE 14. Model predictions with changes in R_{os}. (**A**) Variation of absorptance with respect to variation in reflectance for various R_{os}/R_{is} ratios. (**B**) Temporal variation of absorptance with respect to temporal variations in reflectance for a single cone for various R_{os}/R_{is} ratios. Both (**A**) and (**B**) show a positive correlation in absorptance with respect to the reflectance when the site of variation is R_{os}.

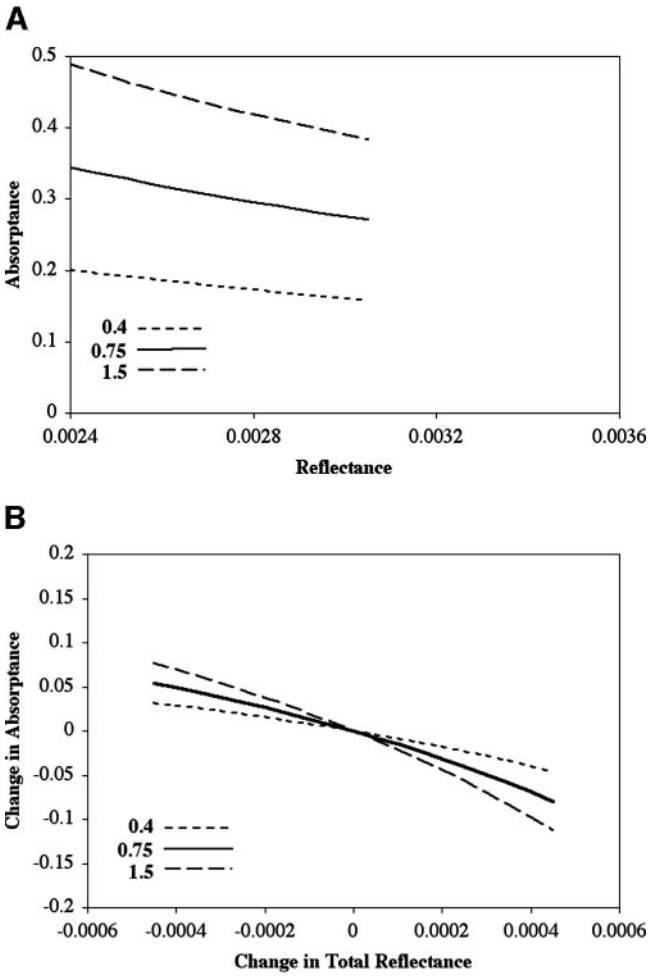

FIGURE 15. Model predictions with changes in R_{is}. (**A**) Variation of absorptance with respect to variation in reflectance for various R_{os}/R_{is} ratios. (**B**) Temporal variation of absorptance with respect to temporal variations in reflectance for a single cone for various R_{os}/R_{is} ratios. Both (**A**) and (**B**) show a negative correlation in absorptance with respect to the reflectance when the site of variation is R_{is}.

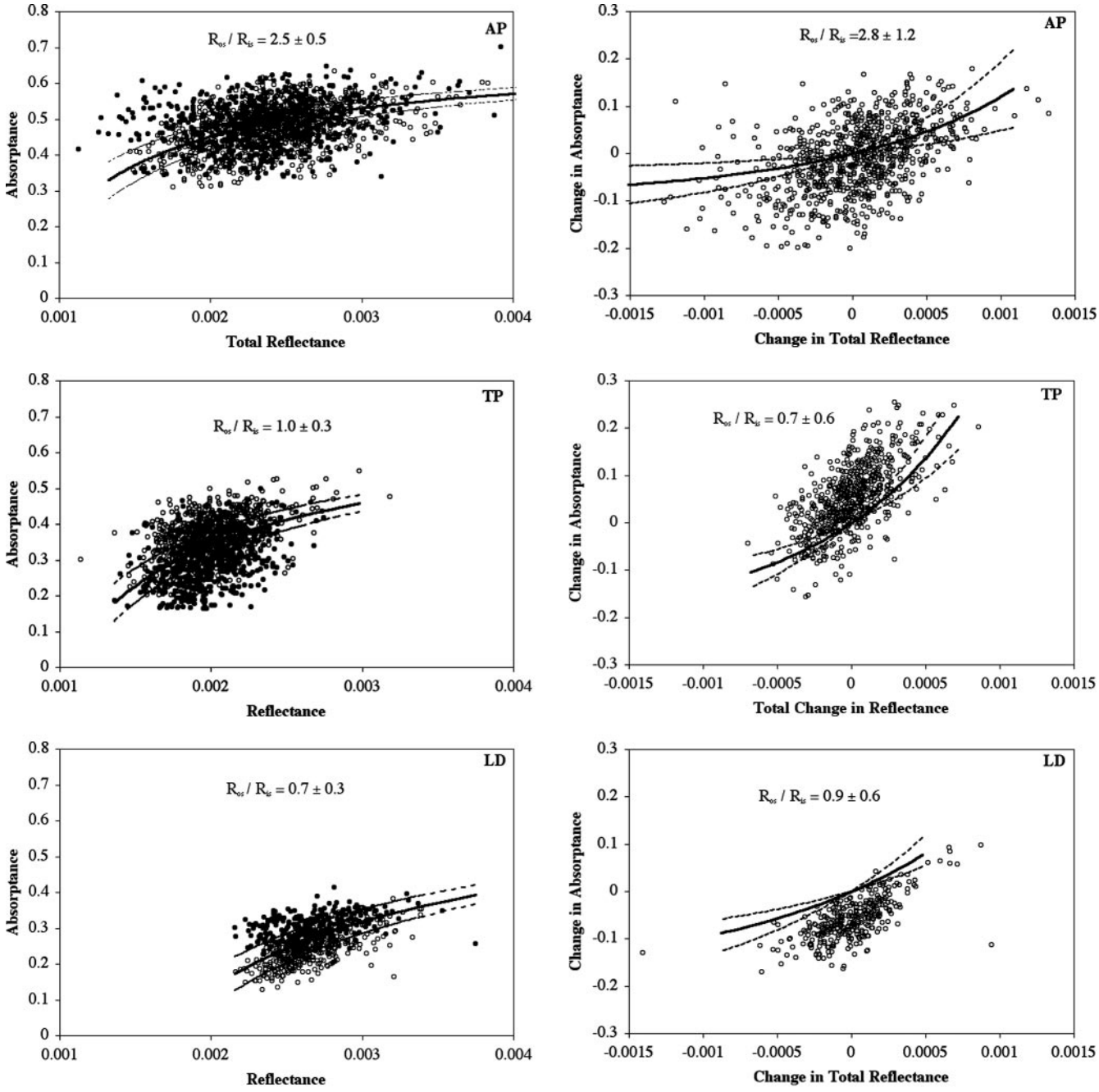

FIGURE 16. Experimental absorptance data for three subjects, AP, TP, and LD. (**A**) Measured absorptance as a function of cone reflectance. Data are shown from day 1 (○) and day 2 (●). The *lines* represent the best fit of the model assuming a change in R_{os}. (**B**) Change in absorptance as a function of change in reflectance from the first to the second day. The *lines* again represent the best fit of the model assuming a change in R_{os}. The ratio of the two reflectances is indicated on the plots.

would account for the experimental data. The curves in Figure 16 were obtained with equations 3, 4, and 5, using a least-squares method, and the confidence intervals for the fits are plotted on the same graphs. A detailed comparison of the shapes of the theoretical curves and the experimental data is not warranted, because of the large variability in the data. However, the similar, positive slope of the data agrees with the theory and supports the view that the changes must be near the outer segment–RPE interface. The fit is even less good for the temporal variation within each cone, in part because there were variations in retinal image quality across days that changed the overall absorptance measures, the absorptance being higher on days when the image quality was better. Thus, the change in absorptance does not have a mean of zero across the cones, and yet the model is constrained to pass through the origin. A more sophisticated model presumably would take retinal image quality into account. Another factor that could have produced a positive slope in these graphs is noise in the fully bleached images, because these images are used to define both the reflectance and the absorptance. However, calculations based on estimates of photon noise showed that the effect is negligible.

Nonetheless, the average ratio of R_{os}/R_{is}, as well as its confidence interval, is given at the top of each graph. This ratio differs substantially from subject to subject. The average ratio across spatial and temporal variation was 2.65, 0.85, and 0.8 for

AP, TP, and LD, respectively. Thus, AP had the greatest fraction of the total reflected light passing through his photopigment followed by TP and then LD. This order also corresponds to that of the quality of the retinal images, with AP having much clearer images of receptors than TP, who in turn had clearer images than LD. The relative reflectance of the two layers seems to have the same order of magnitude as illustrated in another study.[34]

Discussion

A number of models have been developed to describe the reflectance properties of the retina,[35,36] and yet the fractions of light reflected from various layers within the retina are not known in quantitative detail. We have chosen experimental conditions that strongly favor the reflection of light from the photoreceptors alone. These conditions include imaging at high magnification, which reduces contributions from the anterior optics; imaging near the foveal center, which reduces the path length through the inner retina; and the use of 550-nm light, which does not penetrate well into the choroid compared with longer wavelength light. Supporting the view that we had successfully collected light just from receptors, measurements on a single subject, AP, showed that more than 99% of the reflected light was guided by the cones, with only approximately 1% returning in the form of a uniform background. Other studies have reported a more significant amount of diffused component, varying from 17%[21] to 28%,[19] which differs from what we report in this study. However, experimental differences exist between these previous studies as well as our study and a direct comparison is not appropriate at this point. The major difference in our study is the high magnification of the adaptive optics ophthalmoscope that allowed us to study the retinal irradiance of single cones instead of the pupil irradiance or the retinal irradiance of a pool of cones and intercone spacing that cannot be resolved. One might have expected a relatively uniform reflectance from rods superimposed on the more directional cone reflectance. We could not resolve rods in our images and saw little evidence for reflectance from them, probably because of their small size and the fact that, because of their broad tuning, much of the light they return would fall outside the pupil. In AP's eye, we found that the angular tuning was distinctly broader in regions where rods reside between cones rather than being centered on a cone.

Although we seem to have been successful at reducing the reflections from any other layers than the receptors, it is not entirely clear specifically what layers in and around the receptors return light to our CCD camera. Most theories of the origin of the guided light reflected from cones invoke reflectance from a layer at or near the outer segment tip. Gorrand and Delori[37] developed a model based on the waveguide theory and suggested that light is guided toward the RPE through the cone's outer segment. The backscattered light at the outer segment–RPE interface is coupled back in the cone and provides the directional component of the reflected light. This model has been expanded by Marcos et al.[38] to incorporate the scattering of light from different cones. Chauhan and Marshall[39] suggested that the melanin granules might be an especially reflective source in the RPE. Although melanin is highly absorptive, it also has a very high refractive index, so that it can reflect light as does a shiny black marble. There is also some evidence from optical coherence tomography that light is preferentially reflected from the boundary between the inner and outer segments.[40] We have therefore chosen to model our results with two reflectance components from the receptors, one from the inner segment– outer segment interface and one from the outer segment–RPE interface. At least two components are required to account for the fact that our double-pass measurements of photopigment absorptance, like those of practitioners of retinal densitometry, are much lower than the double-pass absorptance expected from the length of cone outer segments and the density of the pigment within them.

Alternative sources of reflection have also been suggested. For example, Van de Kraats et al.[32] proposed a model in which the directional component is reflected back from the outer segment discs and not the outer segment–RPE interface. The model has been extended to include the wavelength dependence of the Stiles-Crawford effect.[41] In their model, the directional component of light may be attributed only to the reflection from the stack of discs in the outer segment, whereas the rest of the reflecting layers contribute to the nondirectional light. In addition, the reflectance of the discs is viewed as a homogeneously distributed reflectance over the full length of the outer segment. As such, changes in the outer segment disc reflectance could cause changes in the intensity of the directional component of light reflected back at the eye. The differences between this model and the model favored in the present study are too small for our experimental data to distinguish. A model that includes reflectance from individual discs can account for the data with a smaller estimate of the stray light that does not pass through any photopigment. The available evidence from the optical coherence tomography would seem to argue against the hypothesis that the discs are reflecting most of the light. However, OCT images are difficult to interpret in the context of this study because, for example, wavelengths are involved. Thus, we cannot exclude the possibility that the reflectance changes we observed are caused by changes in the properties of the discs, such as the spacing between discs, which could change over time and across the retina.

The Site of Spatiotemporal Reflectance Changes

The reflectance changes we have observed in the cone mosaic seem to occur in all cone classes, regardless of the pigment they contain. Based on measurements showing a relative lack of spatial correlation in the reflectance changes of nearby receptors, we conclude that the temporal variations are largely confined to individual receptors, with each receptor operating more or less autonomously of its neighbors. Moreover, the fact that the reflectance changes can be seen in light that is influenced by the waveguide properties of single receptors is also consistent with a cause for the variation that lies within or very near the cone photoreceptor. Light reflected from layers more distant from the outer segment tip, for example, would be less efficiently coupled back into the outer segment for a guided trip back to the pupil.

A promising candidate for the origin of the temporal variations was variation in the pointing direction of single cones, given that it is known that a motor must exist in each cone for steering it toward the incident light. However, observations of the pointing direction of individual cones showed that they were quite stable during a period in which large reflectance changes could be observed. Nor can static disarray between receptors account for the spatial variation in cone reflectance, because previous work has shown that the average disarray of the optical axis of cones has a FWHM of 0.41 mm or less,[9,42,43] which is too small to explain the reflectance variations described in the current study.

Our models of both the spatial and temporal variations in reflectance point to a source that influences mainly the light that passes through the photopigment. Models in which the spatiotemporal variations influence light that does not pass through the photopigment fail to account for the positive correlation between cone photopigment absorptance and cone reflectance. Generally speaking, of course, there are spatial variations in the inner retina, such as those caused by blood vessels that influence the reflectance of cones. However, the

retinal locations we chose were devoid of even the smallest capillaries, reducing the effects of stray light on cone reflectance and making it easier to study the reflectance changes that are intrinsic to cones. Under these circumstances, that the reflectance changes affect light that traversed photopigment also tends to point to a highly local source for the variations, either within the outer segment, or at a reflecting layer that lies very near the outer segment tip.

The temporal variation in the reflectance of single cones is characterized by a slow component in which the reflectance remains correlated up to about 6 hours, with a slight tendency to be negatively correlated between 6 and 24 hours. However, it is also possible to observe quite rapid changes in cone reflectance, which occurs within seconds. Such intrinsic changes in reflectance of single cones may be related to the renewal process of the outer segment discs. Photoreceptors, like most cells, are in a perpetual state of renewing themselves by new membrane assembly as well as outer segment disc shedding. Moreover, the RPE serves many functions, such as the phagocytosis of detached portions of the rod and cone outer segments. Processes extend from the apical surfaces of the RPE cells and engulf a portion of the rod and cone outer segments. Since the discovery of rod and cone renewal,[44–46] many studies have addressed the time course of the process. In most of the species, disc shedding seems to be controlled by a circadian oscillator within the eye that uses endogenous dopamine and melatonin as light and dark signals, respectively. La Vail[47] was the first to report the rhythmic nature of disc shedding in rat rods whereby the majority of discs are detached at light onset. Moreover, it has been observed that most cone outer segment disc shedding takes place 180° out of phase with the major rod-shedding event.[48,49]

We looked at the temporal variation of the variance of the reflectance of a population of cones over a 24-hour period and found that the variance did not exhibit compelling evidence for a circadian rhythm. In addition the autocorrelation curves of the reflectance revealed a noncircadian time signal. Even though this may suggest that disc shedding is not related to the changes in reflectance that we observe, exceptions to the general rules of cone and rod disc shedding have been reported. Rod and cone disc shedding are concurrent in the cat.[50] More important, cone shedding has been reported for both periods of the day in the rhesus monkey.[51] In addition, we cannot rule out the possibility that bleaching the retina every hour for 10 minutes somehow influenced an existing circadian rhythm. Another important aspect of outer segment disc shedding and phagocytosis is the involvement of melanin granules in the renewal process. Various studies have illustrated that the injection of rod outer segments into the subretinal space of rats causes the doubling of the small melanin granules and premelanosomes within the RPE cells compared with areas located at some distance from the site of injection.[52,53] They concluded that melanosomes seem to be involved in the degradation process of outer segment discs during the process of disc shedding and phagocytosis. In addition, Chauhan and Marshall[39] have investigated the relationship between optical coherence tomography images of the retina and the retinal substructure in vitro and in vivo. Their results show that the strongest signal of the outer segment–RPE interface comes from the melanin and lipofuscin granules, whereas there is a weak signal coming from the outer segments themselves. According to our results, most of the changes in directional reflectance may be attributed to the outer segment–RPE interface. Changes in the composition of that interface due to the migration of melanosomes or melanogenesis during disc shedding could explain the changes in reflectance that we observe. Still, disc shedding itself could cause a change in the refractive index of the interface or the waveguide properties of the outer segment.

Even though the reflectance changes that we observed in this study are related to the RPE–outer segment interface, they are not likely to have a direct impact on vision or visual sensitivity. For example, if the changes in reflectance of single cones occur in the RPE–outer segment interface, light has an opportunity to be absorbed on the first pass through the photopigment before reflection from the interface. The visual pigment of the outer segment absorbs incident light with an efficiency of approximately 0.10,[54] which is a conservative number compared with that in another study.[55] Nevertheless, light reflects back from the RPE, but a portion of it scatters around and is not captured by the pigment of the outer segment. The fraction of light that will reflect back from the outer segment–RPE interface will be 0.0009 of the incident light, assuming a reflectance at that interface of approximately 10^{-3}. Thus, if we make the conservative and somewhat unrealistic assumption that all the light returning on the second pass is absorbed, then the total fraction absorbed will be 0.1009. We observe changes in reflectance that are never larger than a factor of 3.5. Such a change would increase the total amount of light absorbed in the second pass to 0.1032 of the incident light. The percentage increase in the light absorbed by the cone caused by this extreme reflectance increase is only approximately 2%, which is below the level of photon noise in single cones even at high light levels. Individual foveal cones are not highly reliable contrast detectors. For example, detecting a 2% change in light intensity in a single foveal cone would require at least 2500 photoisomerizations per integration time. Assuming an integration time of 50 ms, the light intensity would have to correspond to approximately 50,000 photoisomerizations per second which corresponds to a very bright 4,500-troland stimulus.[50] The visual system is capable of detecting 0.5% contrast or less under ideal circumstances, but it requires spatial pooling of signals from many photoreceptors to achieve high contrast sensitivity at low spatial frequencies. The possibility that such changes would be detected is made even more unlikely by the fact that they occur slowly, and adaptation mechanisms make the eye insensitive to slow changes.

However, if the reflectance changes are related to the renewal process of the receptors, then the phenomenon reported herein may make it possible to study disruptions in the disc-shedding process, such as those that occur due to retinitis pigmentosa in the living human eye. In radiometric studies of the normal retina, the temporal changes in reflectance must be taken into account. For example, the classification of cones in images obtained with adaptive optics has so far relied on comparing images taken sequentially in different states of light adaptation.[10,11] The temporal variation in cone reflectance sets a limit on the accuracy with which the pigment in individual cones can be identified and encourages the use of methods in which the images necessary for classification are obtained simultaneously.

Acknowledgments

The authors thank Walter Makous, Andrew Berger, Scott Seidman, and Scott MacRae for helpful assistance during the study.

References

1. Williams DR. Aliasing in human foveal cones. *Vision Res*. 1985;25:195–205.
2. Williams DR. Topography of the foveal cone mosaic in the living human eye. *Vision Res*. 1988;28:433–454.
3. Yellott JI Jr. Spectral analysis of spatial sampling of photoreceptors: topological disorder prevents aliasing. *Vision Res*. 1982;22:1205–1210.
4. Artal P, Navarro R. High-resolution retinal imaging of the living human eye: measurements of the intercenter cone distance by speckle interferometry. *Opt Lett*. 1989;14:1098–1100.

5. Miller DT, Williams DR, Morris GM, Liang J. Images of the cone mosaic in the living human eye. *Vision Res*. 1996;36:1067–1079.
6. Marcos S, Navarro R, Artal P. Coherent imaging of the cone mosaic in the living human eye. *J Opt Soc Am A*. 1996;13:897–905.
7. Liang J, Williams DR, Miller D. Supernormal vision and high-resolution retinal imaging through adaptive optics. *J Opt Soc Am A*. 1997;14:2884–2892.
8. Hofer H, Chen L, Yoon GY, Singer B, Yamauchi Y, Williams DR. Improvement in retinal image quality with dynamic correction of the eye's aberrations. *Opt Express*. 2001;8:631–643.
9. Roorda A, Williams DR. Optical fiber properties of individual human cones. *J Vision*. 2002;2:404–412.
10. Roorda A, Williams DR. The arrangement of the three cone classes in the living human eye. *Nature*. 1999;397:520–522.
11. Roorda A, Metha A, Lennie P, Williams DR. Packing arrangement of the three cone classes in the primate retina. *Vision Res*. 2001;41:1291–1306.
12. Wade AR, Fitzke FW. In-vivo imaging of the human cone photoreceptor mosaic using a confocal LSO. *Lasers Light Ophthalmol*. 1998;8:129–136.
13. Jiang W, Li H. Hartmann-Shack wavefront sensing and control algorithm. *Proceedings of SPIE, Vol. 1271, Adaptive Optics and Optical Structures* 1990;82–93.
14. Alpern M, Maaseidvaag F, Ohba N. The kinetics of cone visual pigments in man. *Vision Res*. 1971;11:539–549.
15. Coletta NJ, Williams DR. Psychophysical estimate of extrafoveal cone spacing. *J Opt Soc Am A*. 1987;4:1503–1513.
16. Krauskopf J. Some experiment with a photoelectric ophthalmoscope in performance of the eye at low luminances. *Symposium Proceedings*. Delft, The Netherlands: Excerpta Medica International Congress Series 125; 1965.
17. Gorrand JM. Directional effects of the retina appearing in the aerial image. *J Opt*. 1985;16:279–287.
18. Blockland GJ. Directionality and alignment of the foveal photoreceptors assessed with light scattered from the human fundus in vivo. *Vision Res*. 1986;26:495–500.
19. Gorrand JM, Delori F. A reflectometric technique for assessing photoreceptor alignment. *Vision Res*. 1995;35:999–1010.
20. Burns SA, Wu S, Delori FC, Elsner AE. Direct measurement of human cone-photoreceptor alignment. *J Opt Soc Am A*. 1995;12:2329–2338.
21. Delint PJ, Berendschot TTJM, van Norren D. Local photoreceptor alignment measured with a scanning laser ophthalmoscope. *Vision Res*. 1997;37:243–248.
22. Stiles WS, Crawford BH. The luminous efficiency of rays entering the eye pupil at different points. *Proc R Soc Lond B*. 1933;112:428–450.
23. Stiles WS. The directional sensitivity of the retina and the spectral sensitivities of the rods and cones. *Proc R Soc Lond B*. 1939;127:64–105.
24. He JC, Marcos S, Burns SA. Comparison of cone directionality determined by psychophysical and reflectometric techniques. *J Opt Soc Am A* 1999;16:2363–2369.
25. Applegate RA, Bonds BA. Induced movement of receptor alignment toward a new pupillary aperture. *Invest Ophthalmol Vis Sci*. 1981;21:869–872.
26. Smallman HS, MacLeod DIA, Doyle P. Realignment of cones after cataract removal. *Nature*. 2001;412:604–605.
27. Rushton WAH. Straylight and the measurement of mixed pigments in the retina. *J Physiol*. 1965;176:46–55.
28. Van Norren D, van der Kraats J. A continuously recording retinal densitometer. *Vision Res*. 1981;21:897–905.
29. Elsner AE, Burns SA, Webb RH. Mapping cone pigment optical density. *J Opt Soc Am A*. 1993;10:52–58.
30. Banks MS, Sekuler AB, Anderson SJ. Peripheral spatial vision: limits imposed by optics, photoreceptors, and receptor pooling. *J Opt Soc Am A*. 1991;8:1775–1787.
31. Bowmaker JK, Dartnall HJ, Lythgoe JN, Mollon JD. The visual pigments of rods and cones in the rhesus monkey, Macaca mulatta. *J Physiol*. 1978;274:329–348.
32. Van de Kraats J, Berendschot TTJM, Van Norren D. The pathways of light measured in fundus reflectometry. *Vision Res*. 1996;36:2229–2247.
33. Ripps H, Weale RA. Analysis of foveal densitometry. *Nature*. 1965;205:52–56.
34. Hammer M, Schweitzer D, Thamm E, Kolb A. Optical properties of ocular fundus tissues determined by optical coherence tomography. *Opt Commun*. 2000;186:149–153.
35. Delori FC, Pflibsen KP. Spectral reflectance of the human ocular fundus. *Appl Opt*. 1989;28:1061–1077.
36. Van Norren D, Tiemeijer LF. Spectral reflectance of the human eye. *Vision Res*. 1986;26:313–320.
37. Gorrand JM, Delori F. A model for assessment of cone directionality. *J Mod Opt*. 1997;44:473–491.
38. Marcos S, Burns SA, He JC. Model for cone directionality reflectometric measurements based on scattering. *J Opt Soc Am A*. 1998;15:2012–2022.
39. Chauhan SD, Marshall J. The interpretation of optical coherence tomography images of the retina. *Invest Ophthalmol Vis Sc*. 1999;40:2332–2342.
40. Drexler W, Morgner U, Ghanta RK, Kartner FX, Schuman S, Fujimoto JG. Ultrahigh-resolution ophthalmic optical coherence tomography. *Nat Med*. 2001;7:502–507.
41. Berendschot TTJM, Van de Kraats J, Van Norren D. Wavelength dependence of the Stiles-Crawford effect explained by perception of backscattered light from the choroid. *J Opt Soc Am A*. 2001;18:1445–1451.
42. MacLeod DIA. Directionally selective light adaptation a visual consequence of receptor disarray? *Vision Res*. 1974;14:369–378.
43. Burns SA, Wu S, He J, Elsner AE. Variations in photoreceptor directionality across the central retina. *J Opt Soc Am A*. 1997;14:2033–2040.
44. Droz B. Dynamic condition of proteins in the visual cells of rats and mice as shown by radioautography with labeled amino acids. *Anat Rec*. 1963;145:157–168.
45. Young RW. The renewal of photoreceptor cell outer segments. *J Cell Biol.* 1976;33:61–72.
46. Hogan MJ, Wood I. Phagocytosis by pigment epithelium of human retinal cones. *Nature*. 1974;252:305–306.
47. La Vail MM. Rod outer segment disc shedding in relation to cycling lighting. *Exp Eye Res.* 1976;23:277–280.
48. Young RW. The daily rhythm of shedding and degradation of rod and cone outer segment membranes in the chick retina. *Invest Ophthalmol Vis Sci*. 1978;17:105–116.
49. O'Day WT, Young RW. Rhythmic daily shedding of outer-segment membranes by visual cells in the goldfish. *J Cell Biol.* 1978;76:593–604.
50. Fisher SK, Pfeffer BA, Anderson DH. Both rod and cone disc shedding are related to light onset in the cat. *Invest Ophthalmol Vis Sc*. 1983;24:844–856.
51. Anderson DH, Fisher SK, Erickson PA, Tabor GA. Rod and cone disc shedding in the rhesus monkey retina: a quantitative study. *Exp Eye Res*. 1980;30:559–574.
52. Peter S, Kayatz P, Heimann K, Schraermeyer U. Subretinal injection of rod outer segments leads to an increase in the number of early-stage melanosomes in retinal pigment epithelial cells. *Ophthalmic Res*. 2000;32:52–56.
53. Schraermeyer U, Peters S, Thumann G, Kociok N, Heimann K. Melanin granules of retinal pigment epithelium are connected with the lysosomal degradation pathway. *Exp Eye Res*. 1999;68:237–245.
54. Barlow HN, Fatt P. Retinal and central factors in human vision limited by noise. In: Barlow HB, Fatt P, eds. *Vertebrate Photoreception.* London: Academic Press; 1977:337–351.
55. Makous WL. Fourier models and the loci of adaptation. *J Opt Soc Am A*. 1997;14:2323–2345.